Supporting Information

An Efficient Biosensor for Monitoring Alzheimer's Disease Risk Factors: Modulation and Disaggregation of Aβ Aggregation Process

Siyue Ma, [a, ‡] Jiabao Qiang, [a, ‡] Linyang Li, [a] Yan Mo, [a] Mengyao She, [a, b] Zheng Yang, [c] Ping Liu, [a] Shengyong Zhang, [a] and Jianli Li [a, *]

[a] Ministry of Education Key Laboratory of Synthetic and Natural Functional Molecule Chemistry, College of Chemistry & Materials Science, Northwest University, TaiBai North Road 229, Xi'an, Shaanxi Province, 710127, PR China.

[b] Key Laboratory of Resource Biology and Modern Biotechnology in Western China, Ministry of Education, The College of Life Sciences, Northwest University, 229 TaiBai North Road, Xi'an, Shaanxi Province, 710069, PR China.

[c] School of Chemistry & Chemical Engineering, Xi'an University of Science and Technology, Yanta Road 58, Xi'an, Shaanxi Province, 710054, PR China.

*Corresponding Author: E-mail: lijianli@nwu.edu.cn

‡ Siyue Ma and Jiabao Qiang contributed equally to this work.

1. Experimental

1.1 Crystal growth and conditions

White single crystals of the probes were obtained at room temperature from the mixed solvents of $CHCl_3$-CH_3CN solution by slow evaporation and then mounted on the goniometer of single crystal diffractometer. The crystal data were collected at 296 K by using Mo Kα radiation by using φ/ω scan mode and collected for Lorentz and polarization effect (SADABS). The structures were solved using the direct method and refined by full-matrix least-squares fitting on F^2 by SHELX-97.

1.2 UV-visible and fluorescence spectral measurements

The stock solutions of the probes were prepared in 100 μmol/L in EtOH-PBS (5:5, v/v) solution. The solutions of the ions were also performed with the salts including KCl, $CaCl_2$, NaCl, $MgCl_2·6H_2O$, $AlCl_3$, $ZnCl_2·6H_2O$, $FeCl_3$, $SnCl_4$, $PbCl_2$, $HgCl_2$, $AgNO_3$, $NiCl_2·6H_2O$, $CoCl_2·6H_2O$, $FeCl_2$, $MnCl_2·5H_2O$, $CrCl_3$, $BaCl_2·2H_2O$, and $CuCl_2·2H_2O$ in EtOH-PBS (5:5, v/v) as 500μmol/L. To determine the spectra properties of the probes, 1.00 mL of the 100 μmol/L solution of the probes, different concentration Cu^{2+} were added to the 10 mL volumetric tubes and diluted to the mark with EtOH-PBS (5:5, v/v) solution. The Absorptions were recorded at 553 nm, and the fluorescence intensities were recorded at 580 nm for both probes with the excitation wavelength at 540 nm.

1.3 Cell imaging

The MCF-7 human breast cancer cell were cultured in Dulbecco's Modified Eagle Medium (DMEM) supplemented with 10% heat in activated fetal bovine serum (FBS) in the humidified atmosphere with 5% CO_2 at 37°C. The cells were cultured for 6 h in treatment conditions until plated on confocal dish. The growth medium was then removed, and the cells were washed with DMEM without FBS and incubated with 50 μmol/L of the probes for 1 h at 37 °C, then washed three times with PBS and imaged. Then the cells were supplemented with 50 μmol/L Cu^{2+} in the growth medium for 30 minutes at 37 °C and imaged. Finally, the cells were supplemented with 50 μmol/L H_2S in the growth medium for 30 minutes at 37 °C and imaged. Bright field and fluorescence images of MCF-7 cells were obtained using an Olympus FV1000 confocal microscope (excited at 543 nm).

1.4 Living mice imaging

Kunming mice were divided into two groups to image Cu^{2+} and H_2S in live mice by subcutaneous injection. The one group was three mice: the first one was given 50 μmol/L probes, the second one was injected with 50 μmol/L probes and then 5 μmol/L $CuCl_2$, the last one was given 50 μmol/L probes and then 50 μmol/L $CuCl_2$. The second group was three mice: the first one was given 50 μmol/L probes, the second one was injected with 50 μmol/L probes and then 50 μmol/L $CuCl_2$, the last one was given 50 μmol/L probes, 50 μmol/L $CuCl_2$ and 50 μmol/L H_2S. Mice were imaged at 0, 1, 5, 10, 20 minutes after a skin-pop injection by using a PerkinElmerLumina LT Serios III, with an excitation of 540 nm and an emission of 580 nm. The study was conducted in accordance with the Experimental Animal Administration regulations issued by the State Committee of Science and Technology of the People's Republic of China.

1.5 Computation details

The Density functional theory (DFT) calculations of the ground state of the probe **S1-S3** and probes-Cu were performed with B3LYP functional with Gaussian 09 Program. The optimization of probe S1-S3 state and probes-Cu state were performed with a basis set consisting of 6-31G* for C, H elements, 6-31 + G** for O, N, Cl elements and DGDZVP for Cu element. The environmental effect was included via PCM model with ethanol as the solvent environment.

2. Calculation of the detection limit of probe S1-S3

$$LOD = \frac{3\sigma}{k}$$

σ is the standard deviation of the blank solution and k is the slope of the linear calibration plot between the fluorescence intensity and the concentration of Cu^{2+}. The calculated LOD of probe **S1-S3** are showed in **Table S-1**.

Table S1. The calculated LOD of probe **S1-S3**

	Probe	**S1**	**S2**	**S3**
LOD	FL(nmol/L)	1.95	1.51	6.62

3. Calculation of the detection limit of probe-Cu^{2+}

$$LOD = \frac{3\sigma}{k}$$

σ is the standard deviation of the blank solution and k is the slope of the linear calibration plot between the fluorescence intensity and the concentration of H_2S. The calculated LOD of probe-Cu^{2+} are showed in **Table S2**.

Table S2. The calculated LOD of probe-Cu^{2+}

	Probe	**S1**	**S2**	**S3**
LOD	FL(nmol/L)	14.8	10.6	16.1

4. Association constant of Cu^{2+} and probe S1-S3

The association constant was determined by Benesi-Hildebrand method as follows:

Probe **S1** is taken as an example. Because of a 1:1 stoichiometry for interaction between probe **S1** and Cu^{2+}, the equilibrium is given by following equation:

$$S1 + nCu^{2+} \overset{K}{\longleftrightarrow} S1 \bullet nCu^{2+} \quad (1)$$

The association constant (k) is therefore expressed as:

$$k = \frac{[S1 \bullet nCu^{2+}]}{[S1][Cu^{2+}]^n} = \frac{[S1 \bullet nCu^{2+}]}{([S1]_0 - [S1 \bullet nCu^{2+}])([Cu^{2+}]_0 - n[S1 \bullet nCu^{2+}])^n} \quad (2)$$

$[S1 \cdot nCu^{2+}]$, [S1], and $[Cu^{2+}]$ represent the equilibrium concentrations of the complex, free **S1**, and free Cu^{2+}, respectively. $[S1]_0$ and $[Cu^{2+}]_0$ are the initial concentrations of **S1** and Cu^{2+}, respectively. If $[Cu^{2+}]_0 >> [S1 \cdot n Cu^{2+}]$, the Eq. 2 can be simplified as follows:

$$k = \frac{[S1 \bullet nCu^{2+}]}{([S1]_0 - [S1 \bullet nCu^{2+}])[Cu^{2+}]_0^{\,n}} \quad (3)$$

Eq. 3 is transformed to:

$$\frac{1}{[S1 \bullet nCu^{2+}]} = \frac{1}{k[S1]_0[Cu^{2+}]_0^{\,n}} + \frac{1}{[S1]_0} \quad (4)$$

Fluorescence intensity is given as follows:

$$F_0 = k_0[S1]_0 \quad (5)$$

$$F = k_0[S1]_0 + k_\infty[S1 \bullet Cu^{2+}] \quad (6)$$

$$F_{\max} = k_0[S1]_{\max} + k_\infty[S1 \bullet Cu^{2+}]_{\max} \quad (7)$$

where, F_0 is the fluorescence intensity of **S1**, F is the fluorescence intensity of **S1** obtained with Cu^{2+}, F_{max} is the fluorescence intensity of **S1** in the presence of excess amount of Cu^{2+}. By means of Eqs. 5, 6 and 7, the following equation is obtained:

$$\frac{F_{\max} - F_0}{F - F_0} = \frac{[S1 \bullet nCu^{2+}]_{\max}}{[S1 \bullet nCu^{2+}]} \quad (8)$$

In the presence of excess amount of Cu^{2+}, $[\mathbf{S1}\cdot nCu^{2+}]_{max}$ is almost equal to $[\mathbf{S1}]_0$. The Eq. 8 can be replaced as follows:

$$\frac{F_{\max} - F_0}{F - F_0} = \frac{[S1]_0}{[S1 \bullet nCu^{2+}]} \quad (9)$$

Using Eq. 4 and 9, the Benesi-Hildebrand equation is obtained as:

$$\frac{1}{F - F_0} = \frac{1}{K(F_{\max} - F_0)[Cu^{2+}]_0^n} + \frac{1}{F_{\max} - F_0} \quad (10)$$

where, F_0 is the fluorescence intensity of **S1**, F is the fluorescence intensity obtained with Cu^{2+}, F_{max} is the fluorescence intensity obtained with excess amount of Cu^{2+}, k is the binding constant, and $[Cu^{2+}]_0$ is the concentration of Cu^{2+} added. Therefore, the binding constant is obtained of 6.05×10^6, 24.13×10^6, 7.70×10^6 for **S1**, **S2** and **S3**, respectively.

5. Optical properties of probe S1-S3

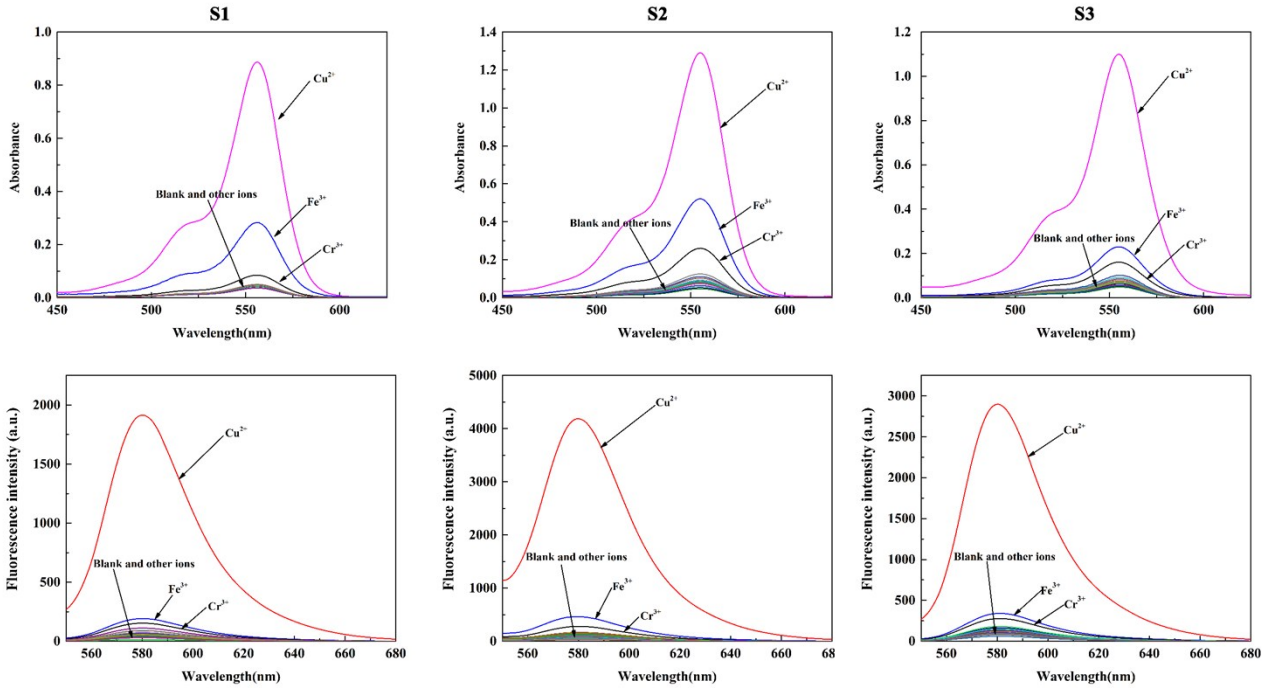

Fig. S1 Absorption and fluorescence spectra of **S1-S3** (10 μmol/L) in EtOH-PBS (5:5, v/v) solution upon addition of various metal ions (20 μmol/L), λ_{ex} = 540 nm.

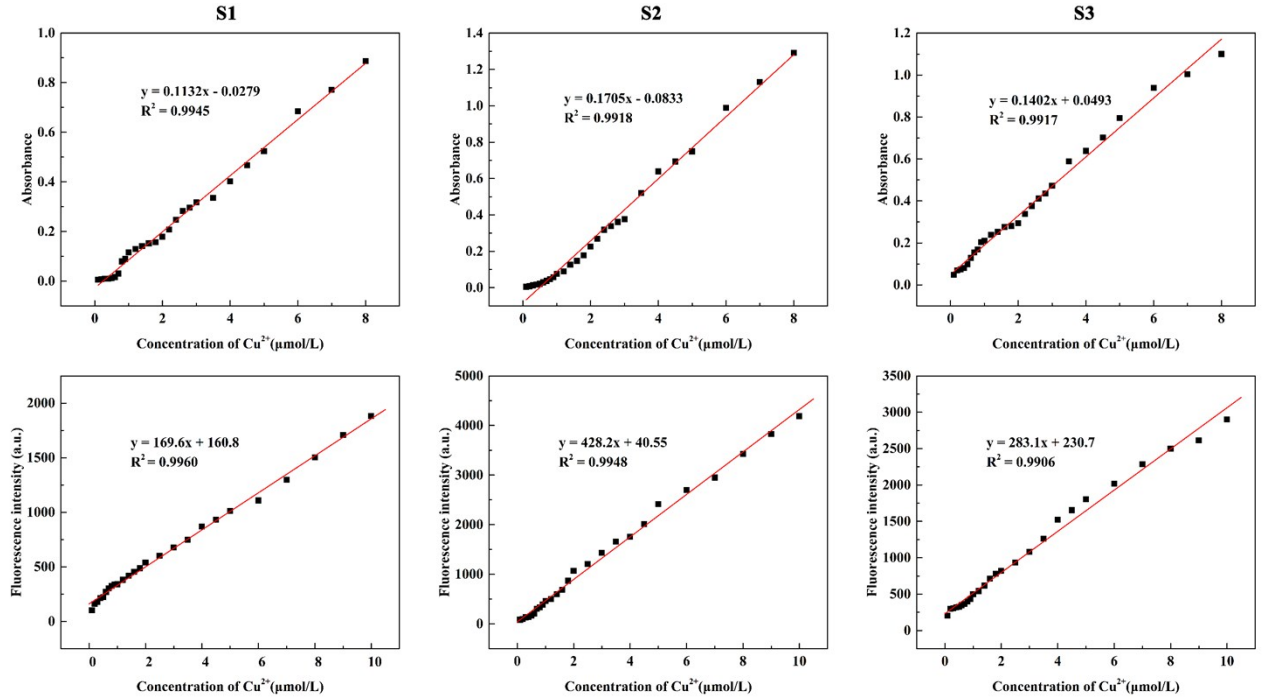

Fig. S2 Absorption of linear of probe **S1-S3** (10 μmol/L) with 0.1-8 μmol/L Cu^{2+}, and fluorescence intensity of linear of probe **S1-S3** (10 μmol/L) with 0.1-10 μmol/L Cu^{2+}, λ_{ex} = 540 nm.

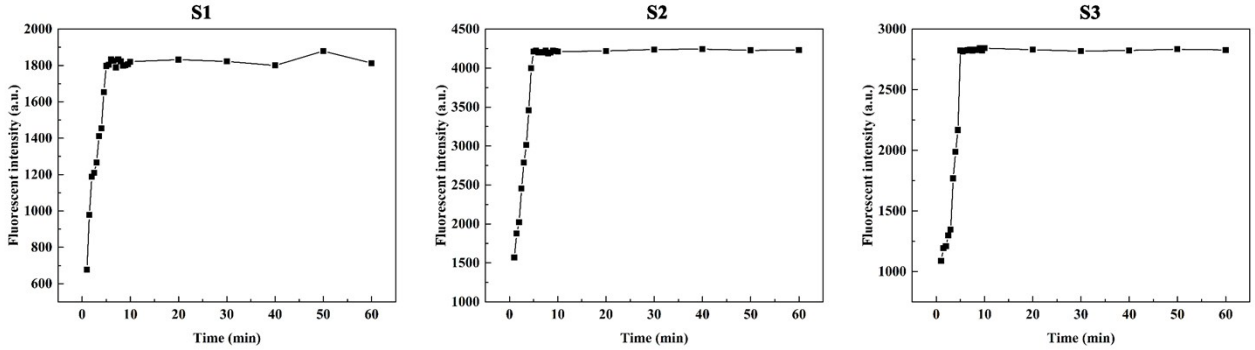

Fig. S3 Time-dependent responses of **S1-S3** with Cu^{2+} in EtOH-PBS (5:5, v/v) solution, λ_{ex} = 540 nm.

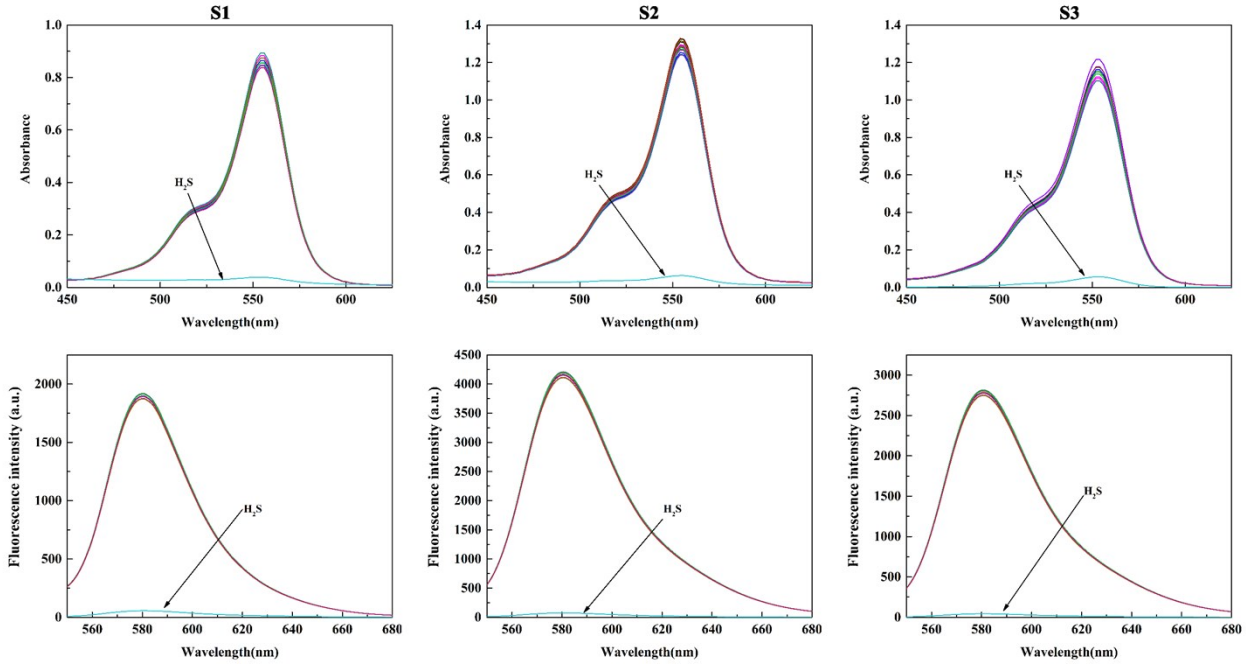

Fig. S4 Absorption and fluorescence spectra of probe-Cu^{2+} (10 μmol/L) in EtOH-PBS (5:5, v/v) solution upon addition of various species (20 μmol/L), λ_{ex} = 540 nm.

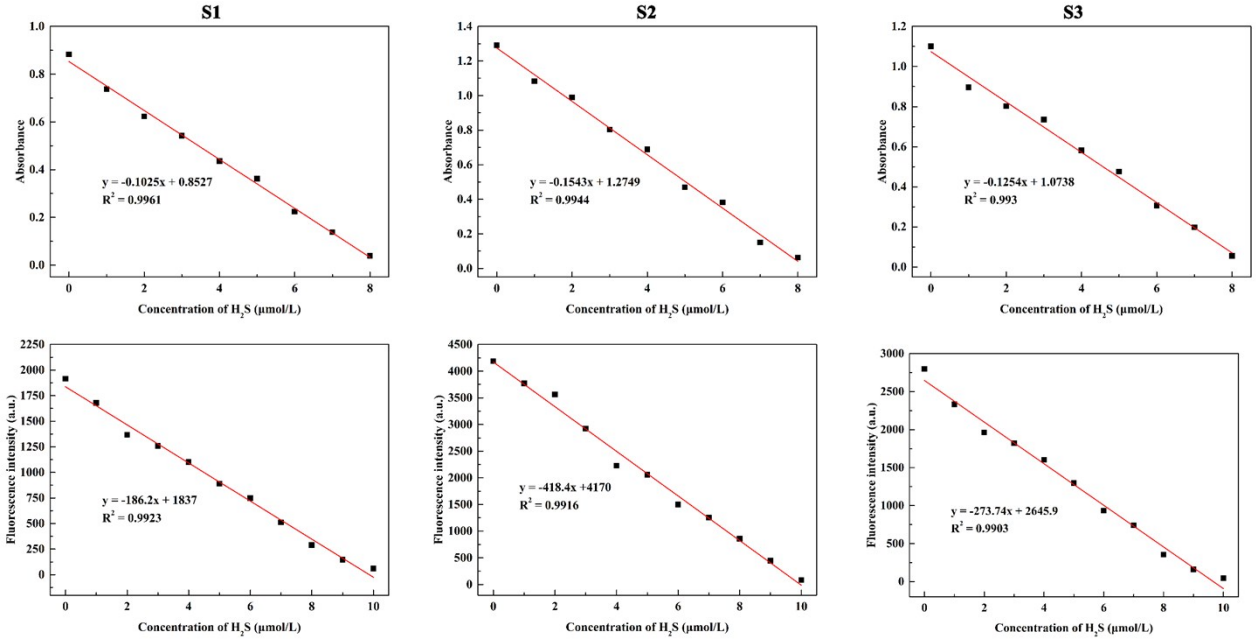

Fig. S5 Absorption of linear of probe-Cu^{2+} (10 μmol/L) with 0-8 μmol/L H_2S, and fluorescence intensity of linear of probe-Cu^{2+} (10 μmol/L) with 0-10 μmol/L H_2S, λ_{ex} = 540 nm.

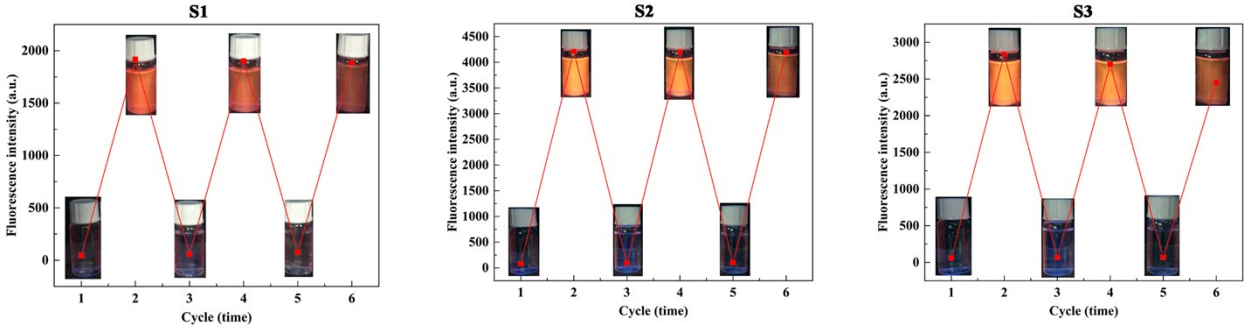

Fig. S6 Fluorescence changes of **S1-S3** at 580 nm upon alternate addition of Cu^{2+} and H_2S in the solution (5:5, v/v, EtOH: PBS, pH 7.4).

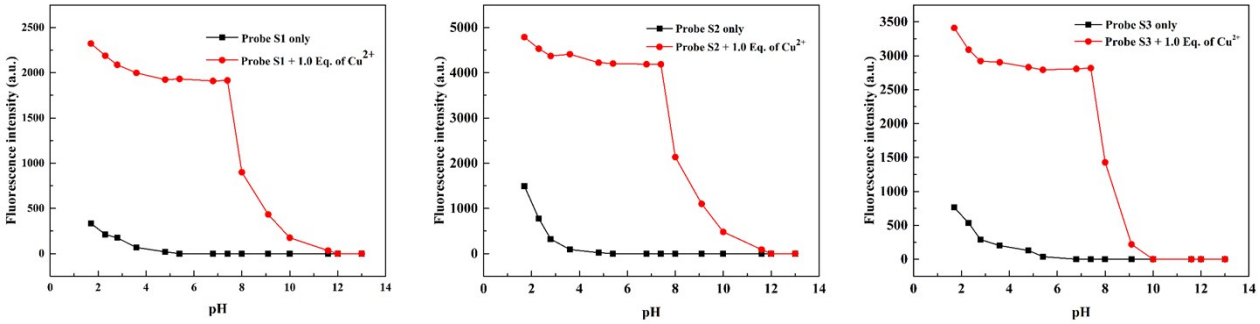

Fig. S7 Fluorescence intensity of **S1-S3** in the absence and presence of 1.0 equiv. of Cu^{2+} in EtOH-PBS (5/5, v/v) solution with different pH conditions, λ_{ex} = 540 nm. The concentration of probe **S1-S3** are 10 μmol/L, and the concentration of Cu^{2+} is 10 μmol/L.

6. Mechanism of S1 responding to Cu^{2+}

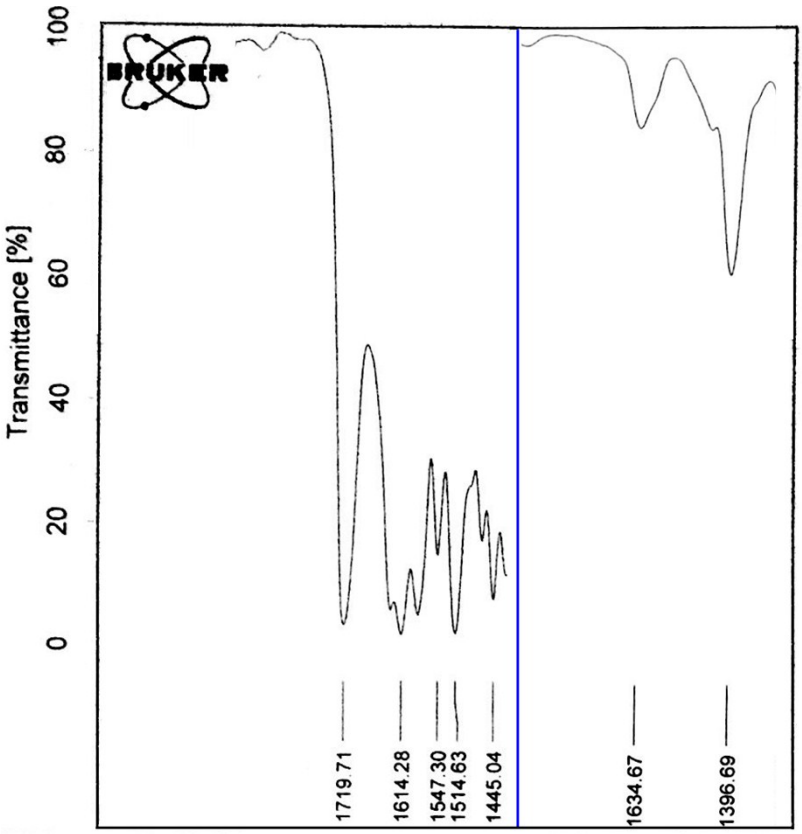

Fig. S8 IR of **S1** and **S1** + $CuCl_2$

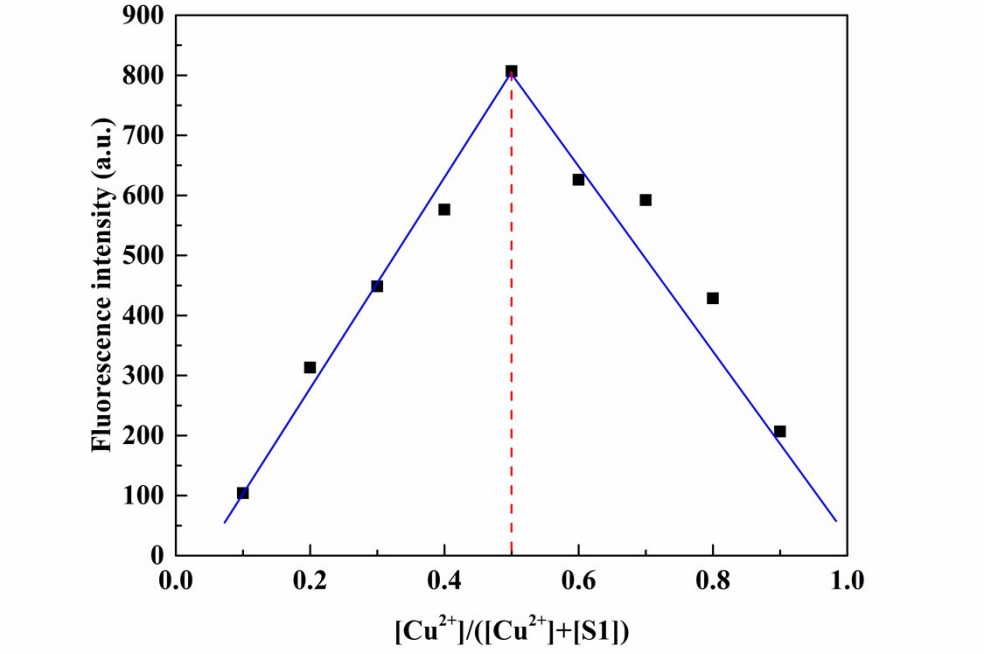

Fig. S9 Job's plot of **S1** with Cu^{2+} in EtOH-PBS (5:5, v/v) solution, λ_{ex} = 540 nm.

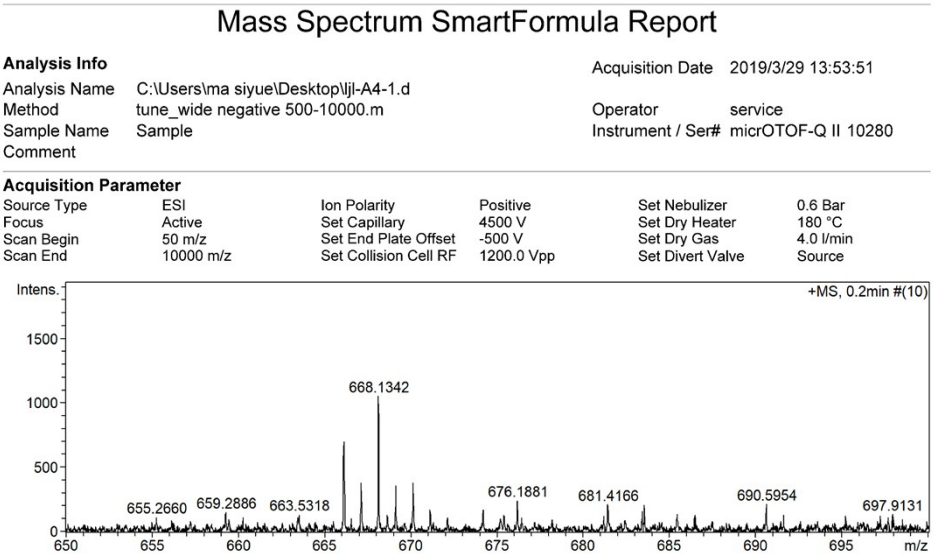

Fig. S10 Mass spectrum of **S1** + $CuCl_2$

7. Theoretical computation

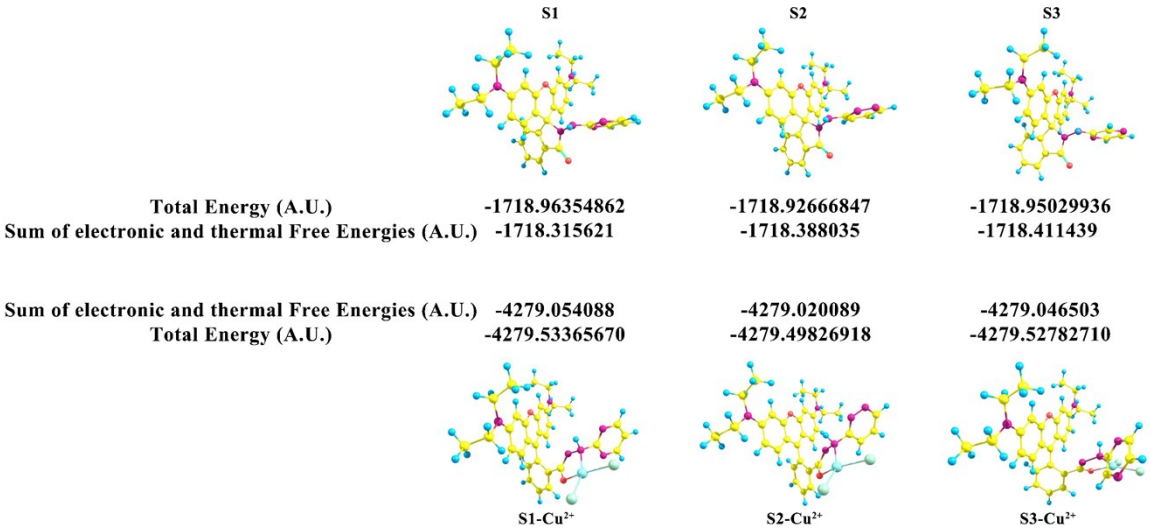

Fig. S11 The optimized structure of the probe **S1-S3** and the complex **S1-S3**-Cu^{2+}.

8. Cell survival rate

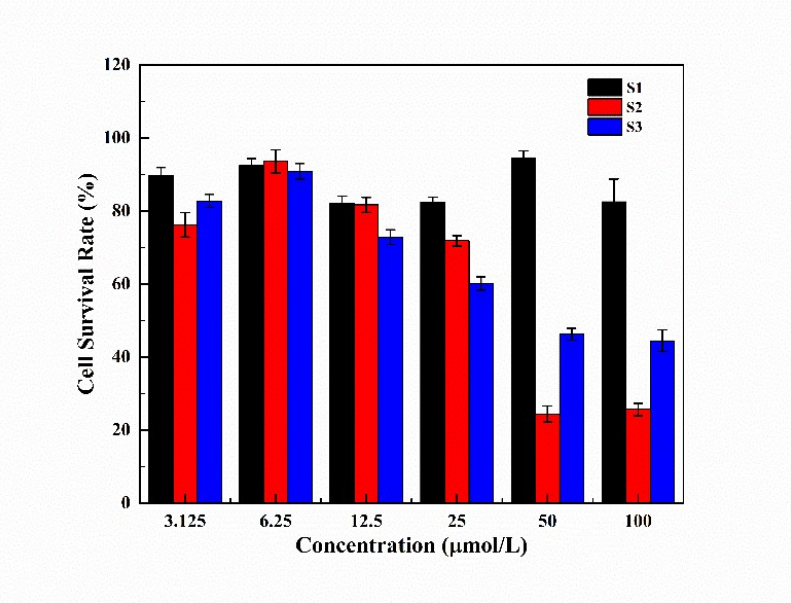

Fig. S12 MTT assay of living cells in the presence of different concentrations of **S1-S3** for 24 h.

9. Blood-brain barrier permeability experiment

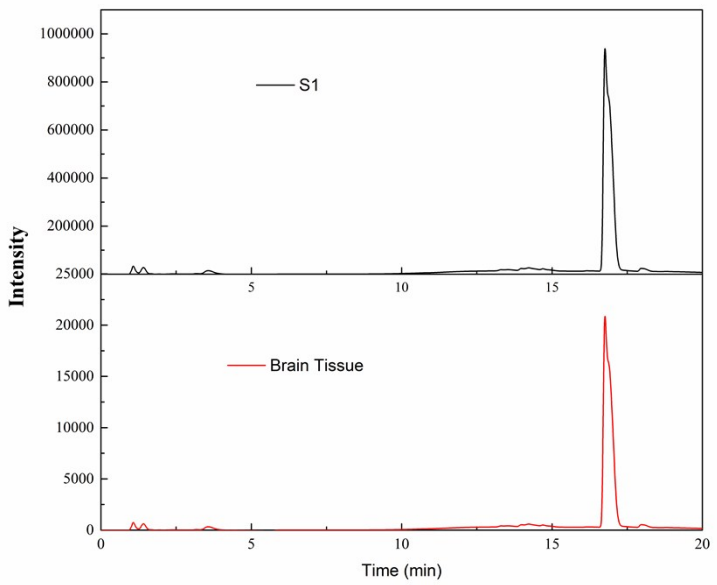

Fig. S13 High performance liquid chromatography experiment of **S1** and brain tissue.

10. IR, NMR and MS spectra of the probes.

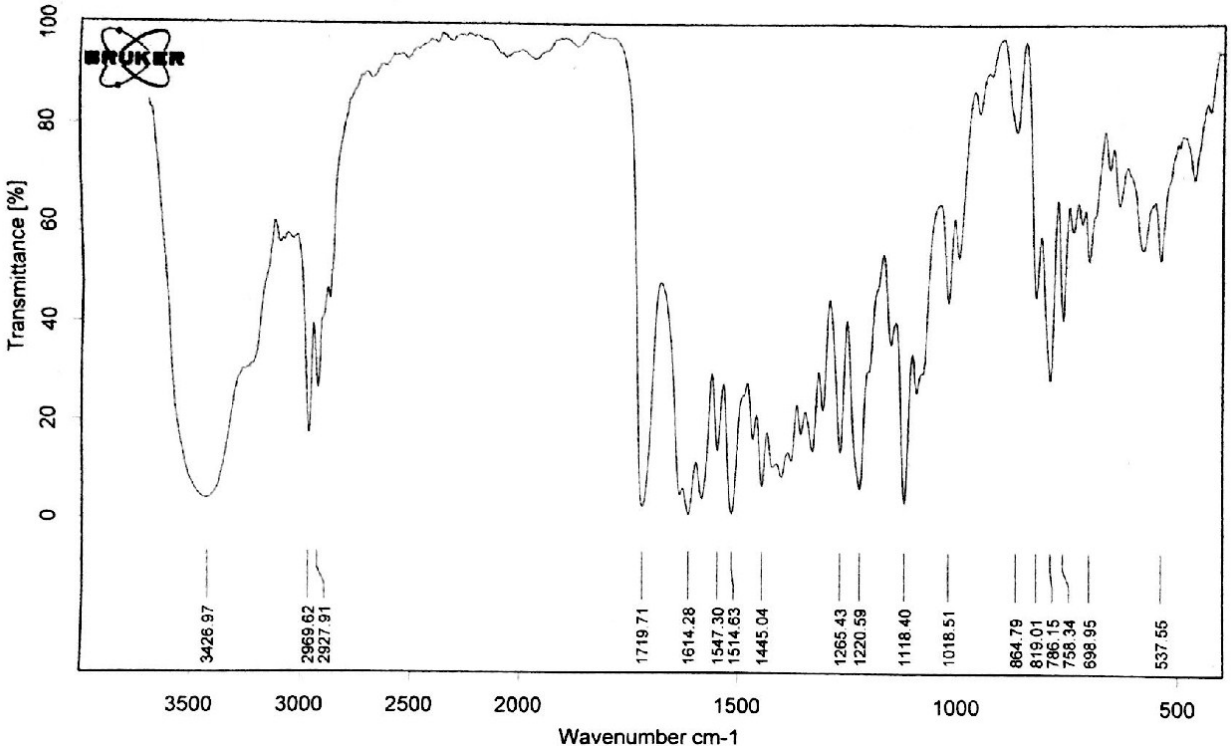

Fig. S14 IR spectrum of **S1** in KBr disks.

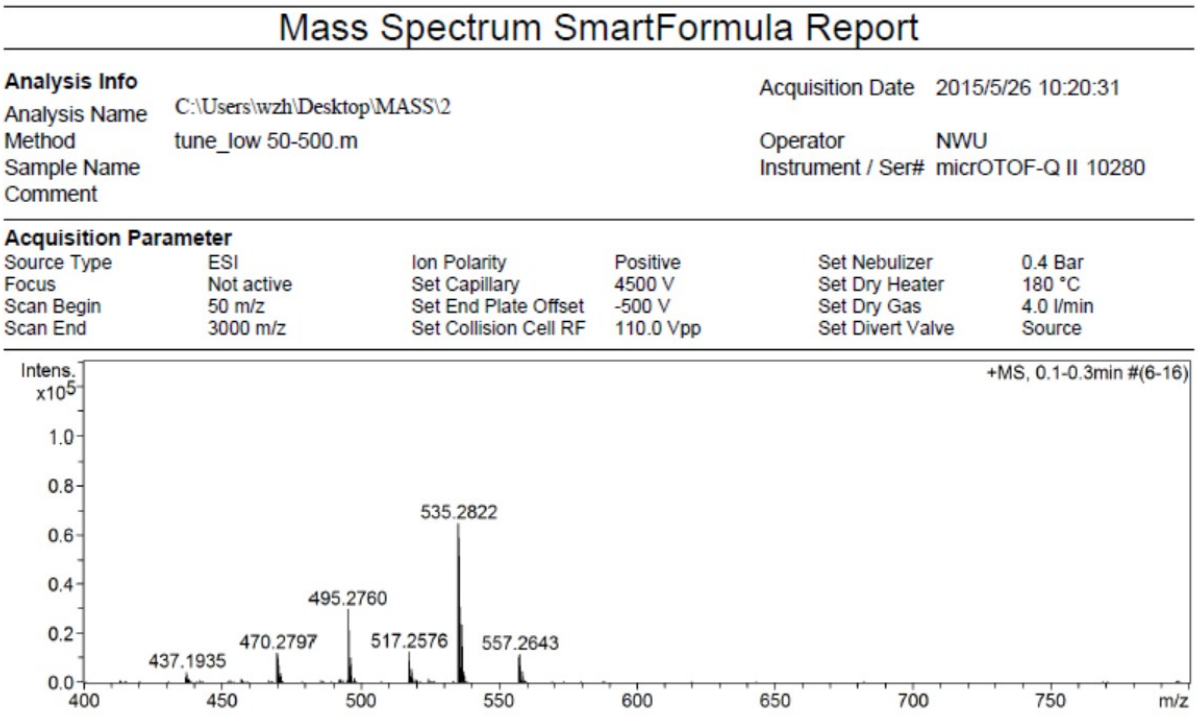

Fig. S15 Mass spectrum of **S1**.

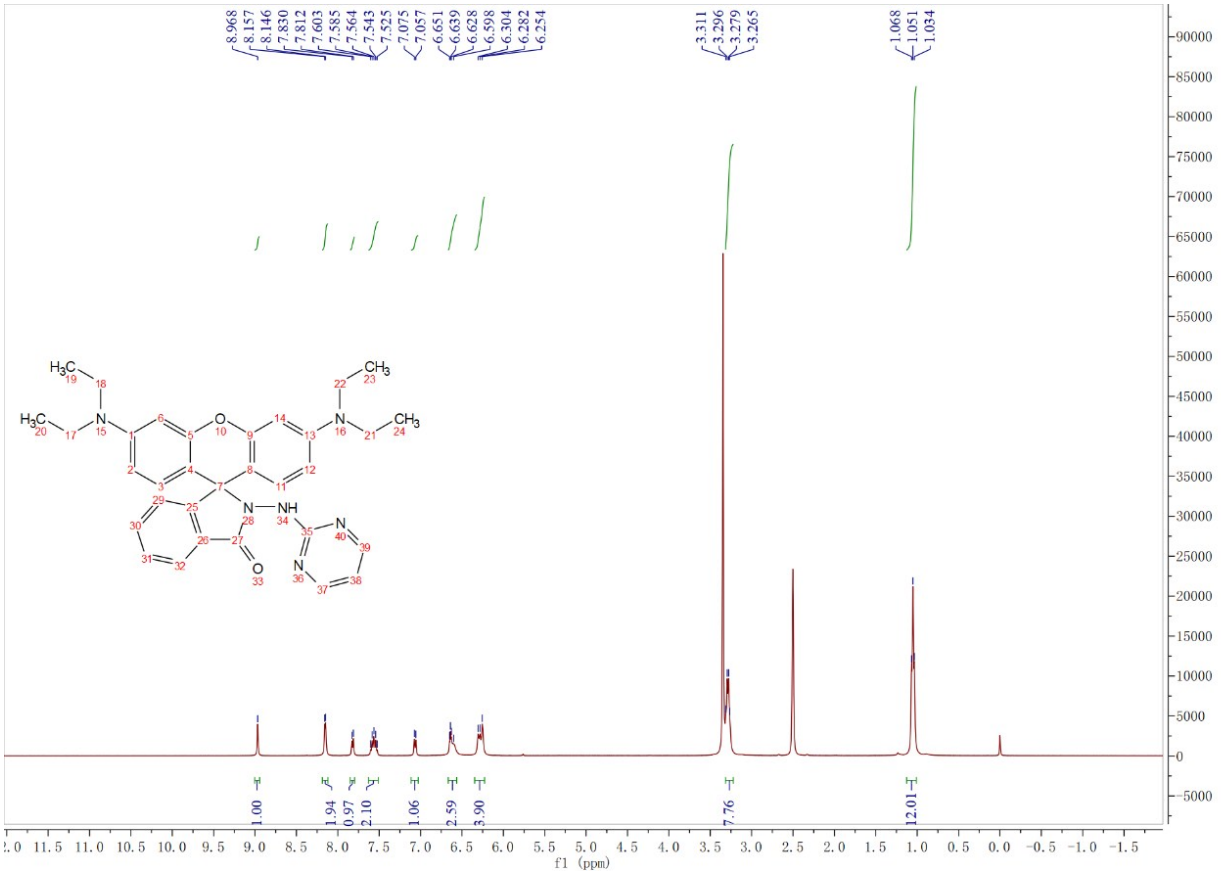

Fig. S16 ^{1}H NMR spectrum of **S1** in DMSO.

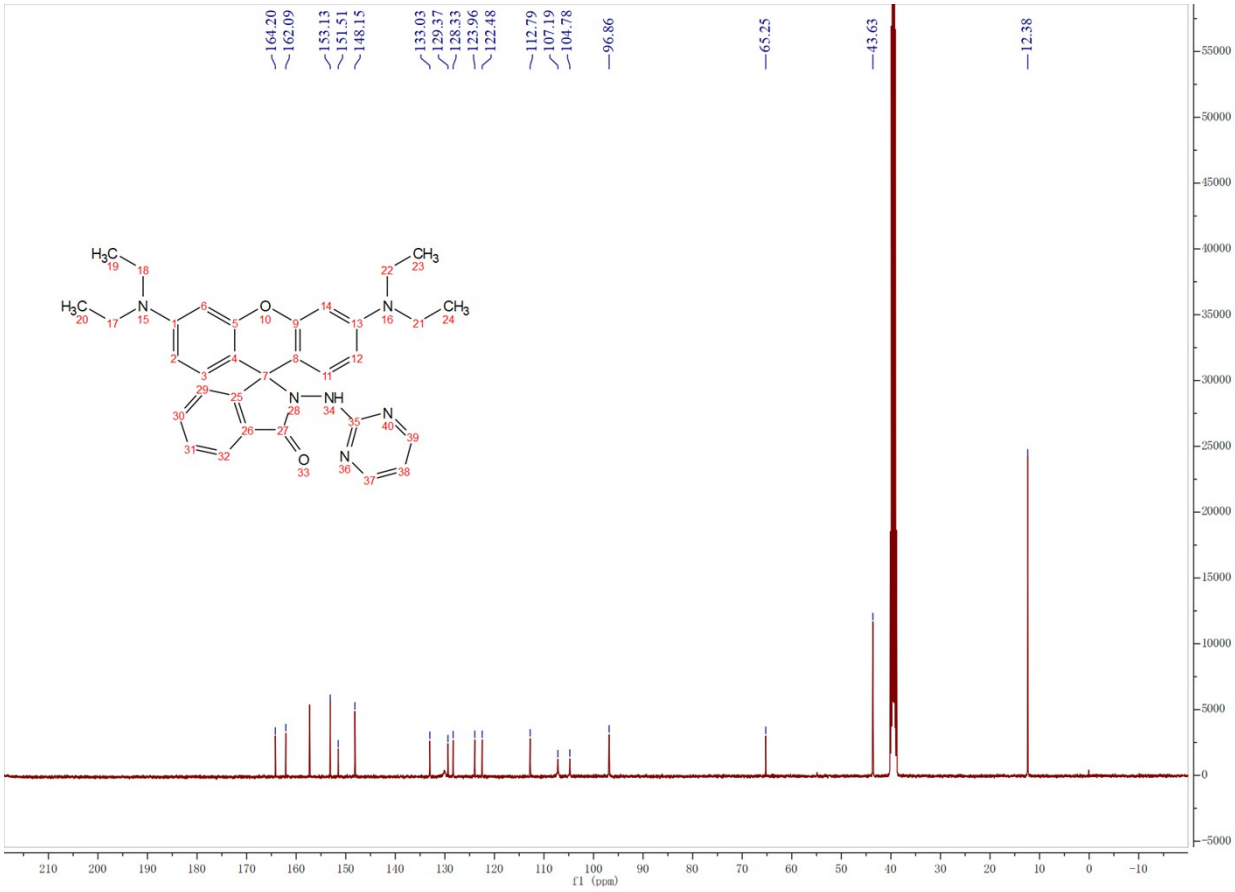

Fig. S17 ^{13}C NMR spectrum of **S1** in DMSO.

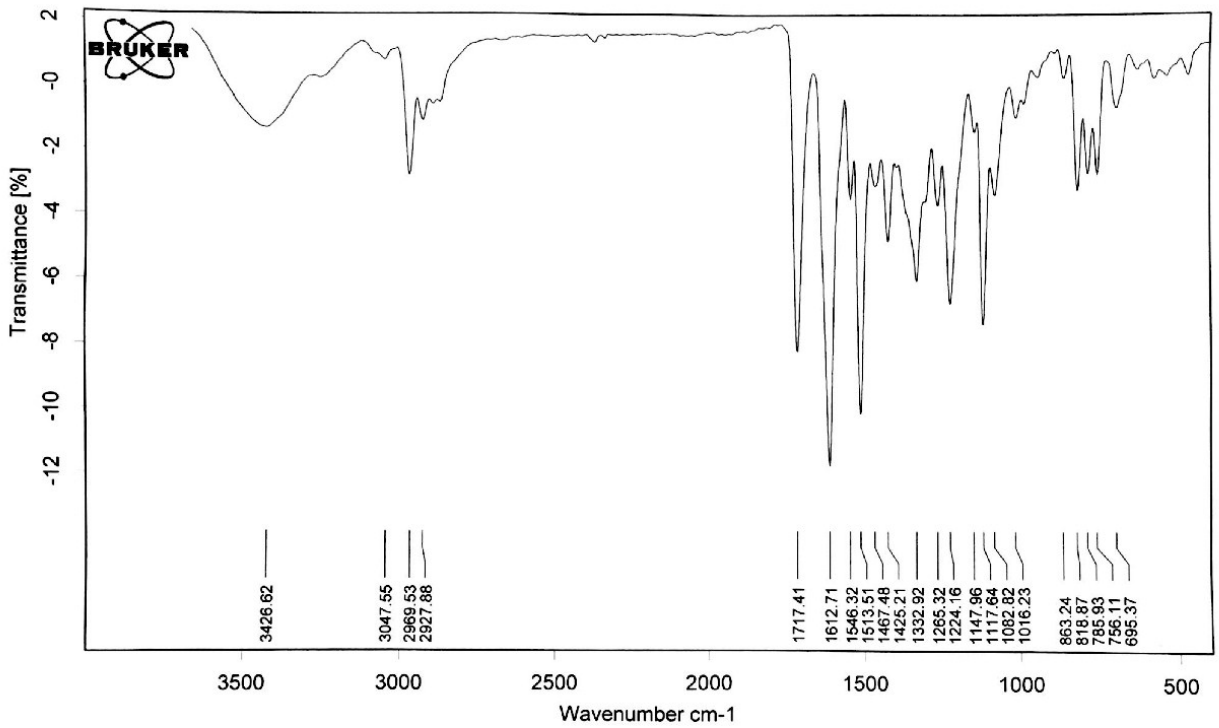

Fig. S18 IR spectrum of **S2** in KBr disks.

Mass Spectrum SmartFormula Report

Analysis Info

Analysis Name	C:\Users\wzh\Desktop\lijianli-804-3.d	Acquisition Date	2015/12/10 9:25:21
Method	tune_low 50-500.m	Operator	NWU
Sample Name		Instrument / Ser#	micrOTOF-Q II 10280
Comment			

Acquisition Parameter

Source Type	ESI	Ion Polarity	Positive	Set Nebulizer	0.4 Bar
Focus	Not active	Set Capillary	4500 V	Set Dry Heater	180 °C
Scan Begin	50 m/z	Set End Plate Offset	-500 V	Set Dry Gas	4.0 l/min
Scan End	3000 m/z	Set Collision Cell RF	110.0 Vpp	Set Divert Valve	Source

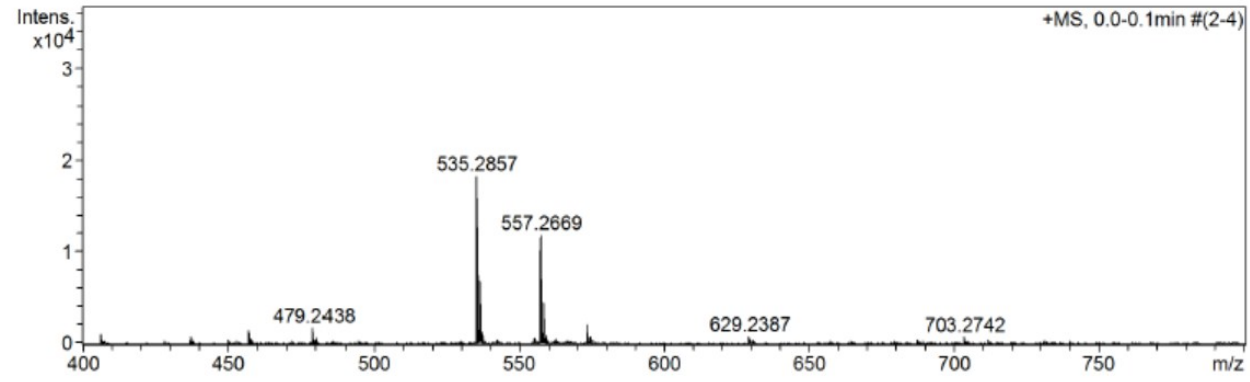

Fig. S19 Mass spectrum of **S2**.

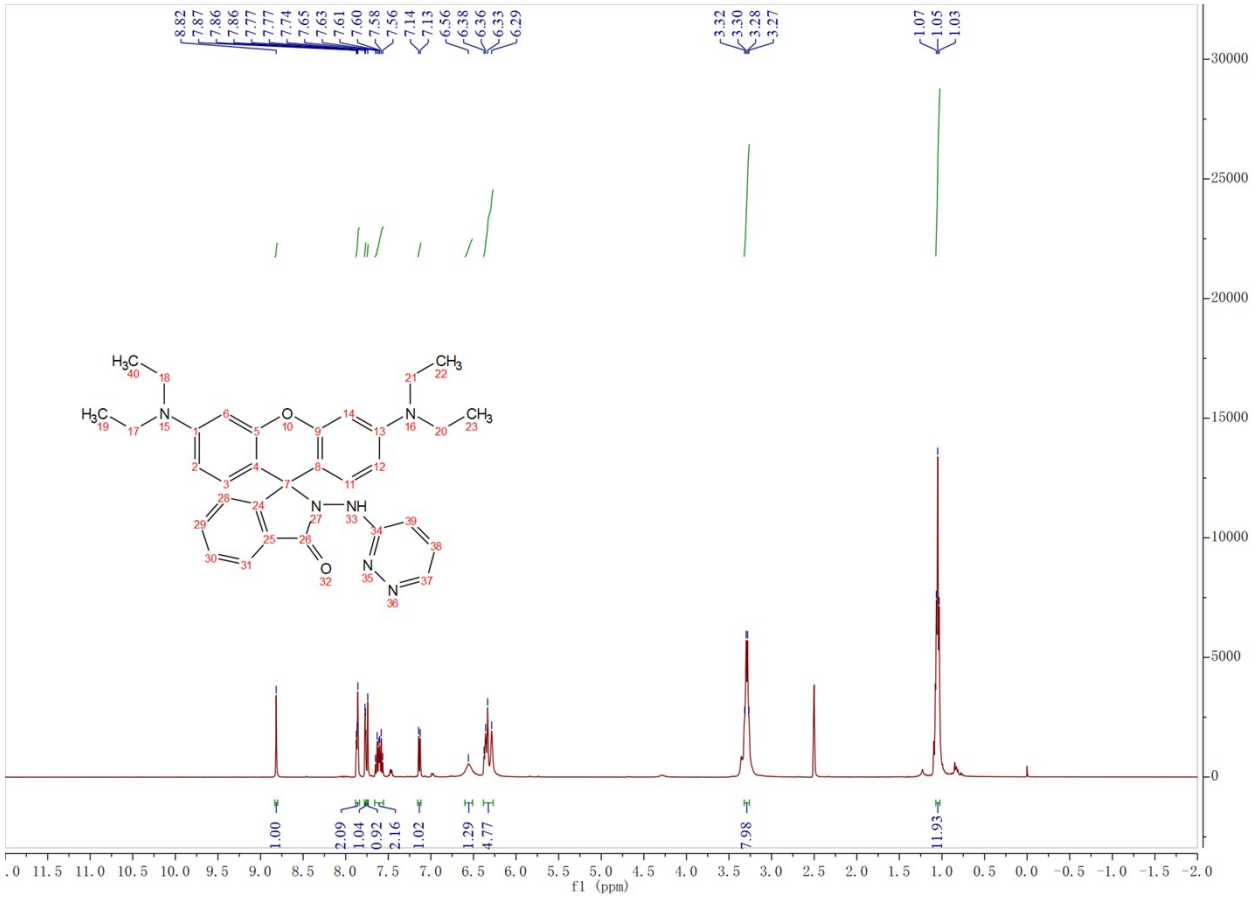

Fig. S20 ^{1}H NMR spectrum of **S2** in DMSO.

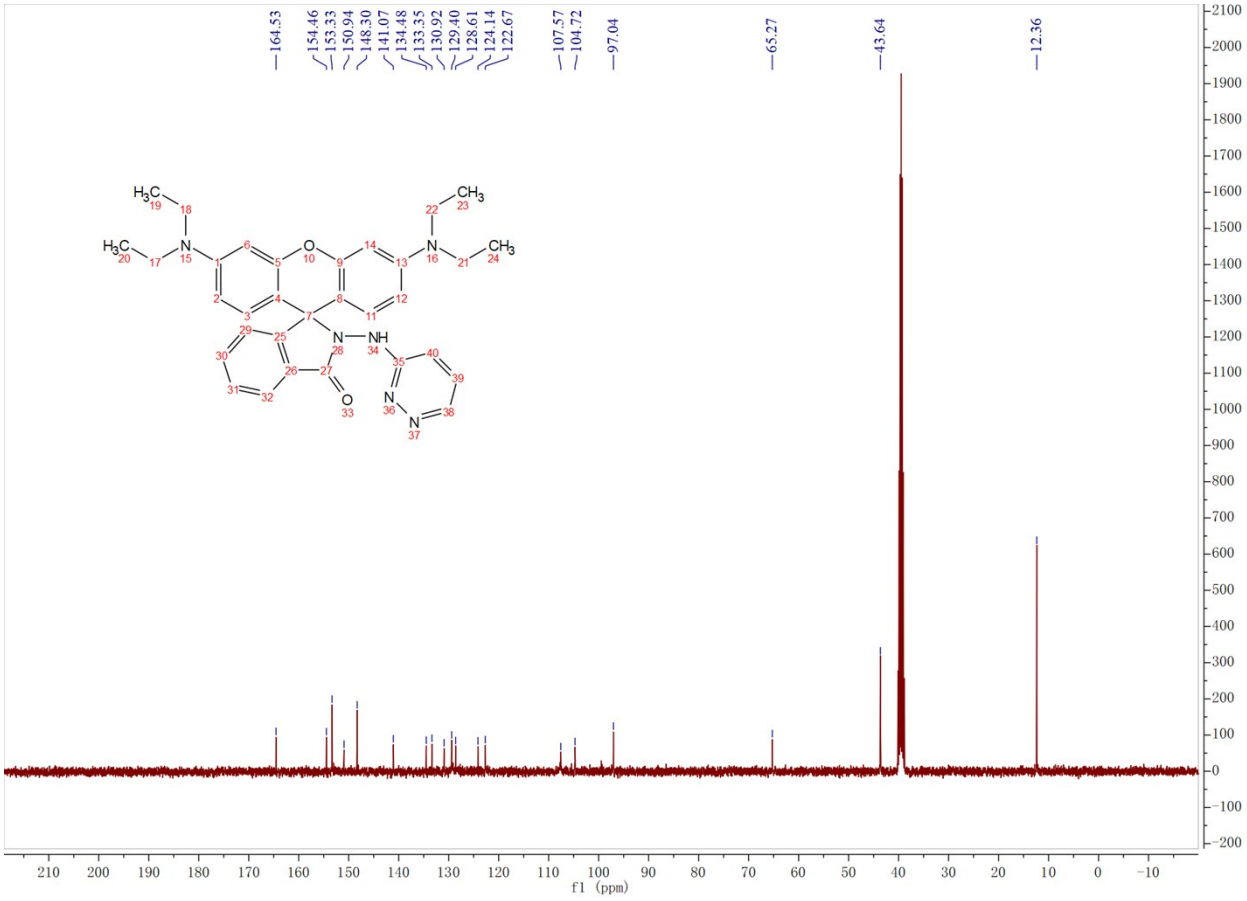

Fig. S21 ^{13}C NMR spectrum of **S2** in DMSO.

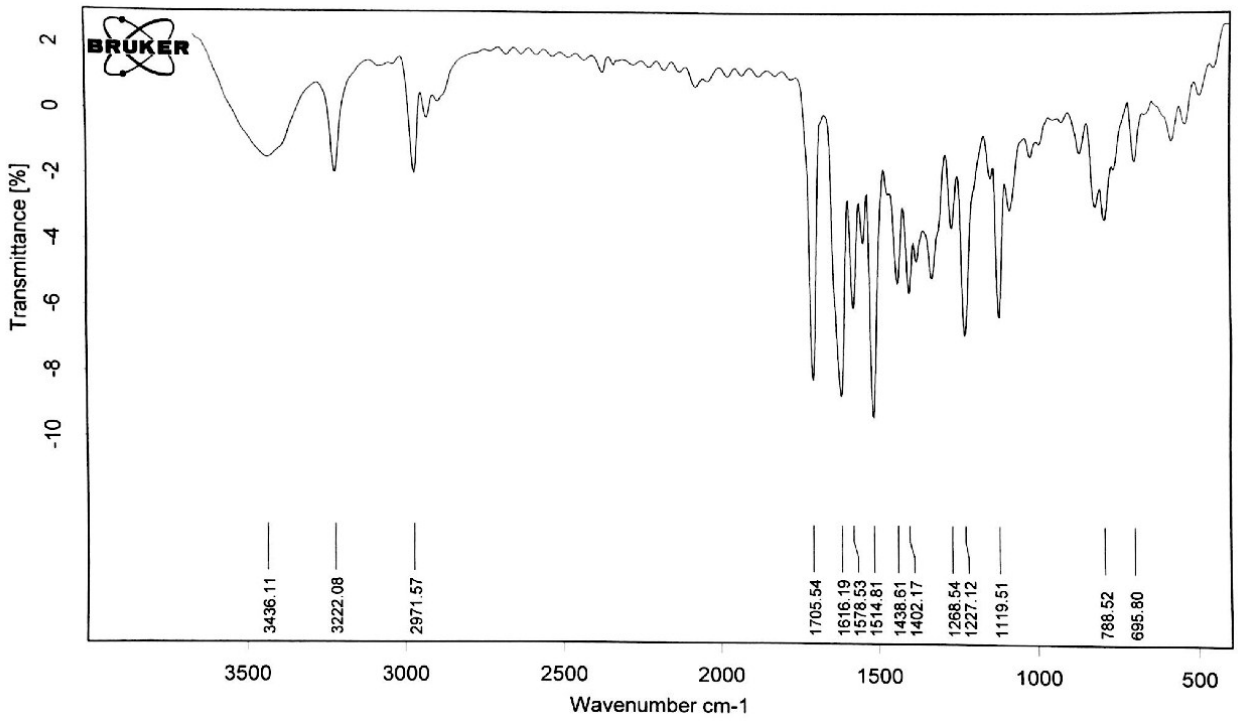

Fig. S22 IR spectrum of **S3** in KBr disks.

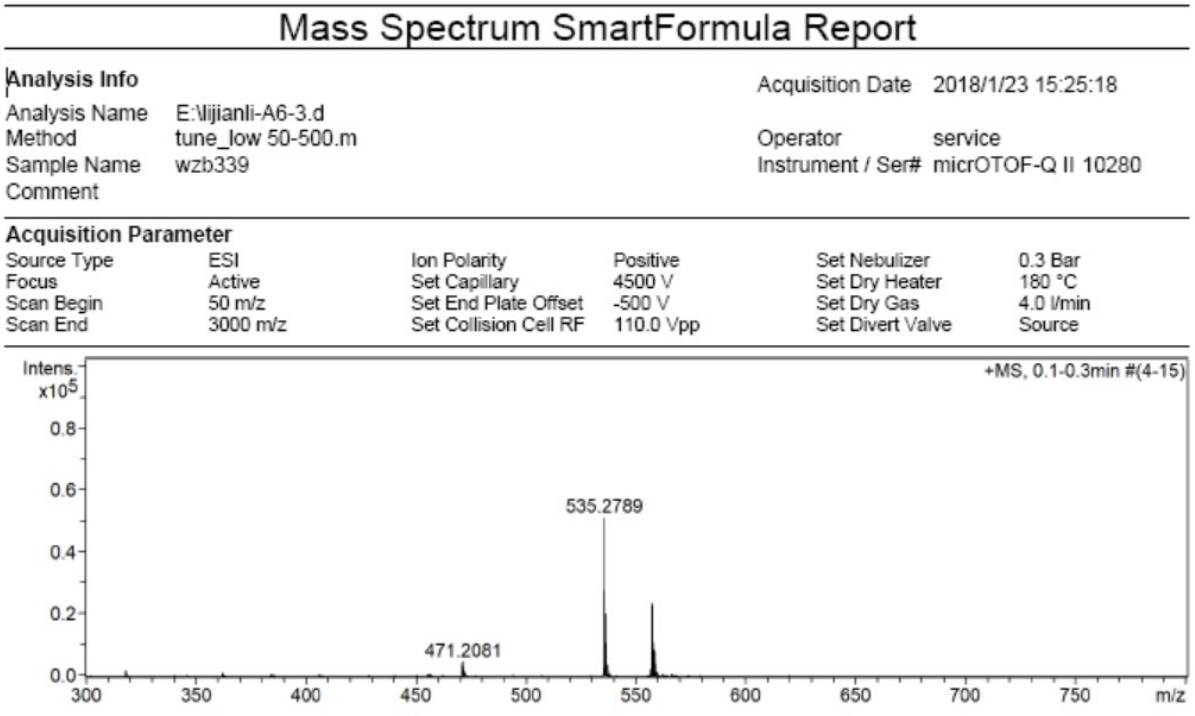

Fig. S23 Mass spectrum of **S3**.

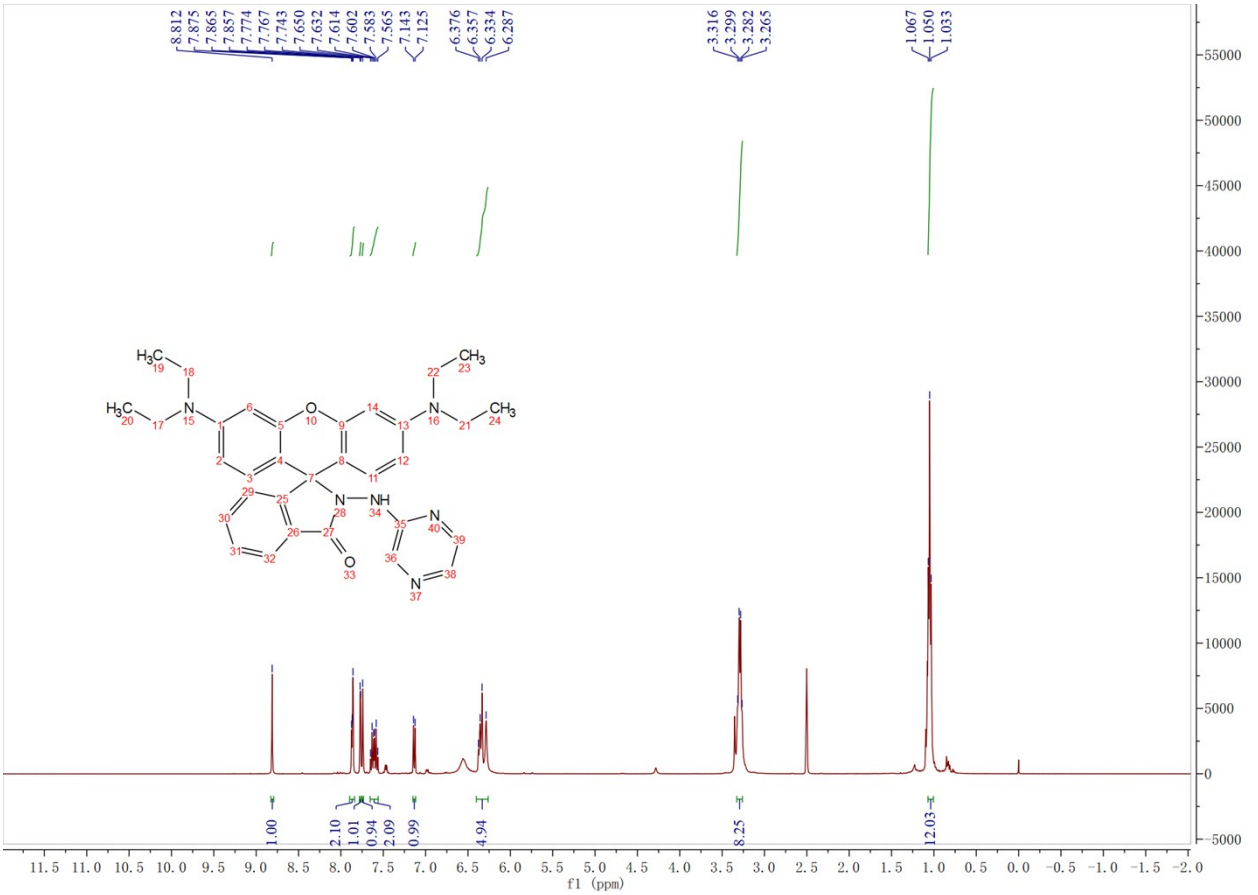

Fig. S24 ^{1}H NMR spectrum of **S3** in DMSO.

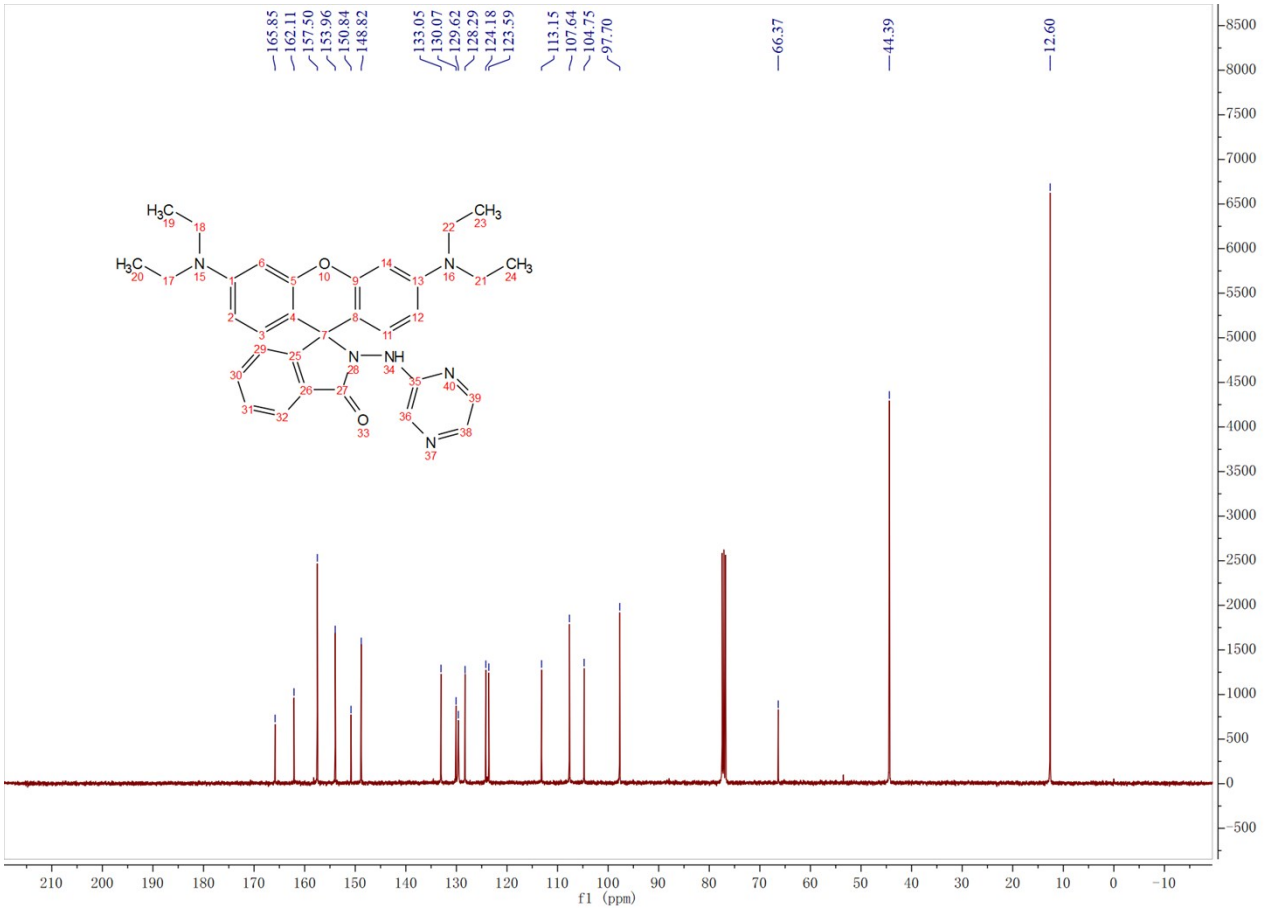

Fig. S25 ^{13}C NMR spectrum of **S3** in $CDCl_3$.